SF2A 2025
A. Siebert, K. Baillié, M. Béthermin, F. Cantalloube, E. Josselin, N. Lagarde, J. Malzac, J. Richard, L. Selliez, O. Venot (eds)

HCN VUV ABSORPTION CROSS SECTION AT HIGH TEMPERATURE FOR WARM EXOPLANETS

A. Collado[1], O. Venot[1], B. Fleury[1], Z. Perrin[1], R. Roméo[2], Y. Bénilan[3], N. Fray[3], A. Jolly[3], X. Landsheere[1], S. Triquet[1], M. Feingesicht[1] and P. Zapf[1]

Abstract. With the new generation of telescopes such as JWST, ARIEL, and PLATO, the characterization of exoplanet atmospheres has become a major objective. The interpretation of exoplanet atmospheres relies on the use of atmospheric models that require accurate and appropriate physico-chemical data as inputs. Among these data, ultraviolet (VUV) absorption cross sections are essential to describe radiative transfer and photodissociation reactions in kinetic models. Here we present new experimental measurements of the VUV absorption cross section of hydrogen cyanide (HCN) in the 115 - 200 nm range, for temperatures between 300 and 700 K. Our results show that the absorption cross section increases with temperature especially at long wavelengths ($\lambda > 180$ nm). This temperature dependence affects atmospheric modeling results, leading to variations in the abundance of HCN itself as well as other key species through changes in their photodissociation pathways.

Keywords: Exoplanet atmospheres, laboratory astrophysics, spectroscopic techniques, modelling

1 Introduction

The characterization of exoplanet atmospheres has considerably progressed with the advent of new space observatories such as JWST (Gardner et al. 2023) and future missions like ARIEL (Tinetti et al. 2018) and PLATO (Rauer et al. 2025). The in-depth interpretation of these observations relies on thermo-photochemical models that describe the chemical composition of planetary atmospheres. Such models require a large set of physico-chemical data, including VUV absorption cross sections, to compute photodissociation rates. Most of the existing VUV cross section databases were obtained at ambiant temperature (300 K)(Heays et al. 2017). Yet, hot exoplanets exhibit much higher temperatures, typically ranging from 500 to 2000 K. Using ambiant temperature cross sections to simulate atmosphere with such conditions introduces strong uncertainties in model predictions. Previous works have already demonstrated the importance of temperature-dependent cross sections, with absorption cross sections increasing by several orders of magnitude when the temperature rises (CO_2, Venot et al. 2013, 2018; C_2H_2, Fleury et al. 2025). Hydrogen cyanide (HCN) is a key molecule for planetary atmospheres (Fortney et al. 2019) as it is the simplest C/H/N bearing species. It is involved in photochemistry, and its abundance is of particular interest for C-rich atmospheres with HCN becoming a major species (Rocchetto et al. 2016). Nevertheless, no measurements of HCN VUV absorption cross sections at high temperature were available until now. The present study addresses this gap by measuring the absorption cross section of HCN in the 115 - 200 nm range, for temperatures between 300 and 700 K, and by quantifying the impacts of these new data on atmospheric modeling.

2 Methods

2.1 *Synthesis of HCN*

HCN is not commercially available. For this reason, HCN was synthesized in the laboratory through reaction 2.1 :

$$\mathrm{NaCN} + \mathrm{CH_3(CH_2)_{16}COOH} \longrightarrow \mathrm{HCN} + \mathrm{Na[CH_3(CH_2)_{16}COO]} \tag{2.1}$$

[1] Université Paris Cité and Univ Paris Est Creteil, CNRS, LISA, F-75013 Paris, France
[2] Astrophysics Group, University of Exeter, EX4 4QL Exeter, UK
[3] Univ Paris Est Creteil and Université Paris Cité, CNRS, LISA, F-94010 Créteil, France

This reaction occurs under vacuum conditions (1×10^{-3} mbar), producing dry HCN, which was condensed in a flask cooled with liquid nitrogen (77 K). The purification of the sample was achieved by fractional condensation: a first slush at 178 K and a second one at 233 K were carried out to remove potential impurities (CO_2 and H_2O).

2.2 Measurement of VUV absorption cross section

HCN absorption spectra were measured using a VUV spectroscopy platform developed at the Laboratoire Interuniversitaire des Systèmes Atmosphériques (LISA, France). The gas was irradiated with a deuterium lamp and the emitted light was dispersed by a 1 m McPherson 225 UHV monochromator. The absorption cell, made of quartz, was heated by a tube furnace, with the temperature monitored by three thermocouples. Spectra were measured in the range 115 to 200 nm divided into 9 smaller ranges of ∼10 nm each and recorded several times (5 - 8) at pressures ranging from 1×10^{-3} to 4×10^{2} mbar with an instrumental spectral resolution of 0.065 nm.

2.3 Calculation of the absorption cross section

The absolute absorption cross section of HCN was derived from the Beer-Lambert law:

$$\sigma(\lambda, T) = \frac{1}{nL} \times \ln\left(\frac{I_0}{I}\right)$$

The absorption cross section $\sigma(\lambda$, T) is expressed in cm^2, with L being the optical path length (cm), n the gas density (cm^{-3}), I_0 and I the transmitted intensities through the empty and filled cell, respectively. Assuming ideal gas behavior, $n = \frac{P}{k_B T}$ with P (Pa), T (K), and k_B the Boltzmann constant. Data were processed using an in-house Python code: noisy and saturated points were removed, and the spectra were averaged every 0.02 nm with the remaining points to obtain the final HCN absorption cross sections.

3 Results

3.1 Photoabsorption of HCN

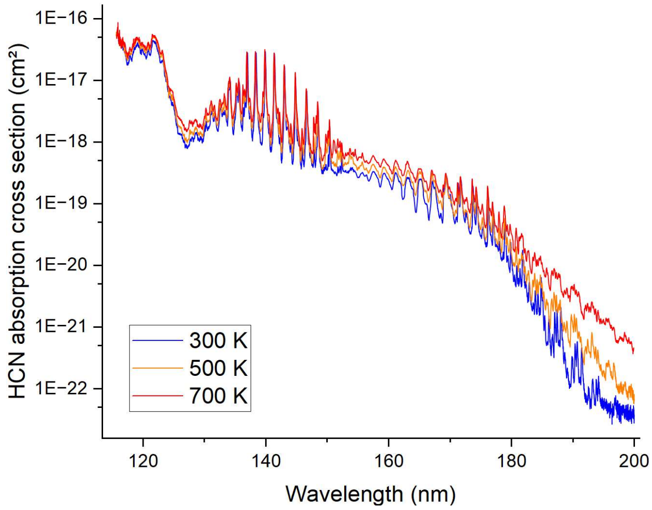

Fig. 1: Measured HCN absorption cross section between 115 and 200 nm, at 300 K (*blue*), 500 K (*orange*) and 700 K (*red*).

The absorption cross section of HCN was measured at 300, 500, and 700 K (Fig. 1). At higher temperatures, we observe an increase of the continuum, leading to an overall rise in absorption. This effect becomes particularly noticeable at wavelengths above 160 nm, with the greatest increase (up to one order of magnitude) reached near 200 nm. In addition to the continuum increase, the structure of the absorption bands evolves with temperature. We distinguish two types of bands:

- Cold bands, corresponding to transitions from the vibrational ground state of the electronic ground state.

- Hot bands, transitions where the initial state is a thermally populated vibrationally excited level.

While the intensity of cold bands is only weakly affected by temperature, hot bands become increasingly prominent as temperature rises. The observed behavior can be explained by the redistribution of the molecular population among vibrational states as temperature increases. At higher temperatures, excited vibrational levels of the fundamental electronic state are more populated, which enhances the probability of hot transitions.

3.2 Modeling

3.2.1 Chemical composition

To quantify the impact of these warm HCN absorption cross sections on atmospheric composition, we performed 1D thermo-photochemical simulations of a fictive exoplanet atmosphere. To do so, we used the 1D kinetic model FRECKLL (Al-Refaie et al. 2024) coupled with a kinetic network for C,H,O,N species (Venot et al. 2020). The planetary parameters are summarized in Table 1.

Table 1: Planetary parameters

Metallicity (solar)	C/O	Radius (R_J)	K_{zz} (cm^2s^{-1})	d (ua)
10	1.5	0.56	1×10^7	0.047

For the VUV cross sections of HCN, we constructed a composite VUV absoption cross section by combining data previously measured at BESSY synchroton data (2007, unpublished) in the 80 - 115 nm range with our newly acquired measurements in the 115 - 200 nm range. At room temperature (300 K), we merged the two datasets (80 - 115 nm and 115 - 200 nm at 300 K) to obtain a continuous spectrum. To build the '700 K' dataset, we used the same 80 - 115 nm data at 300 K, but combined it with our new 115 - 200 nm measurements recorded at 700 K. Two identical simulations were carried out, except for the HCN absorption cross section used: one using the spectrum measured at 300 K, and the other one using that at 700 K. Except the HCN VUV absorption cross section, all the other absorption cross sections used correspond to ambiant temperature.

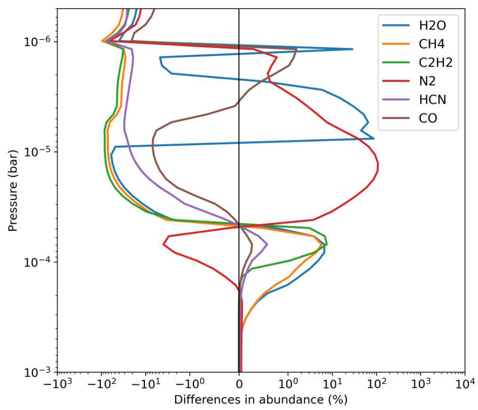

Fig. 2: Differences in abundances (%) between the results obtained using $\sigma_{HCN}(\lambda,700)$ and $\sigma_{HCN}(\lambda,300)$.

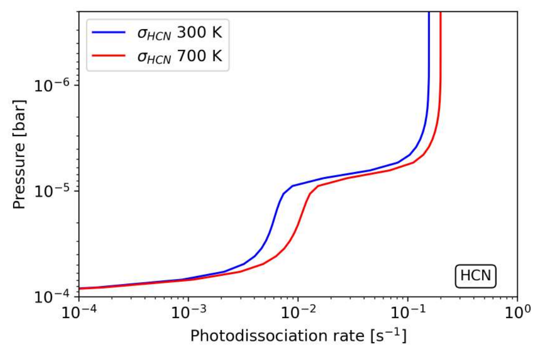

Fig. 3: Photodissociation rate of HCN using $\sigma_{HCN}(\lambda,700)$ (*red*) and $\sigma_{HCN}(\lambda,300)$ (*blue*)

As expected, we have a significant impact on the vertical abundance of HCN with an average decrease of 12.56% (for the pressure range shown in Fig. 2) for pressure lower than 1×10^{-4} bar. Interestingly, the effect of the temperature-dependent HCN cross section extends to other molecules. Molecules such as H_2O, C_2H_2, or N_2 exhibit strong abundance variations, with a significant decrease of some species at a certain altitude. We calculated the relative deviation of abundances $(((y^{700} - y^{300})/y^{300}) * 100)$ reaching values as large as - 95.64% (for CH_4) or + 108.01% (for N_2) depending on altitude (Fig. 2). This shows that a single updated dataset in the photochemical network can induce significant shifts. The decrease in HCN abundance is consistent with the increase in its VUV absorption, which enhances its photodissociation rate (see Fig.3). Specifically, the rate is roughly doubled near 5×10^{-4} bar, and remains higher at lower pressures throughout the upper atmosphere.

3.2.2 Opacity

The increase of HCN absorption at high temperature has also an impact on atmospheric opacity. As can be seen in Fig. 4, there are almost no changes in the 115 - 140 nm region, but in the 150 - 190 nm range, where HCN contributes strongly, we observe a significant increase in its contribution to the total opacity at $\tau = 1$. In this wavelength region, C_2H_2 also absorbs stellar flux. However, since HCN captures a larger fraction of the photons when using the cross section at 700 K rather than at 300 K, C_2H_2 receives less flux and thus contributes less to the overall opacity. This competition results in a small decrease in the C_2H_2 photodissociation rate (Fig. 5), illustrating a shielding effect of HCN on other absorbers.

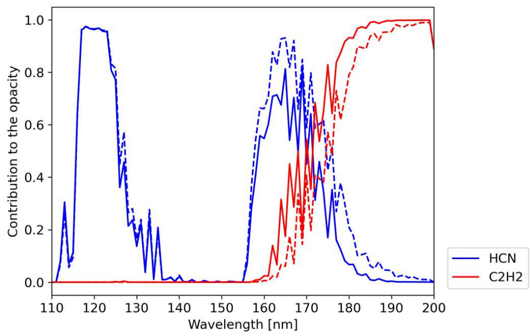

Fig. 4: Contribution of HCN and C_2H_2 to the opacity $\sigma_{HCN}(\lambda,300)$ (full lines) and $\sigma_{HCN}(\lambda,700)$ (dotted line)

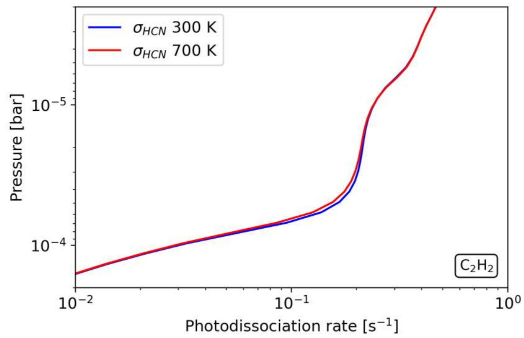

Fig. 5: Photodissociation rate of C_2H_2 in the simulation using the $\sigma_{HCN}(\lambda,300)$ (*blue*) and $\sigma_{HCN}(\lambda,700)$ (*red*).

4 Conclusions

We experimentally investigated the thermal dependence of HCN by measuring its VUV absorption cross section at 300, 500, and 700 K over the 115 - 200 nm range, and evaluated the implications of these new data for atmospheric modeling. Absorption increases overall with temperature, an effect most pronounced at longer wavelengths ($\lambda > 180$ nm), where it can reach nearly an order of magnitude. Incorporating these data into the kinetic model FRECKLL to simulate a fictive exoplanet atmosphere results in an average decrease of 12.56% in HCN abundance in the top of the atmosphere, a doubling of its photodissociation rate near 5×10^{-4} bar, and strong variations in other species (C_2H_2, CH_4, N_2, H_2O), up to $\pm100\%$. Enhanced HCN absorption also affects the opacity, competing with C_2H_2 in the 150-190 nm range and reducing its photodissociation. This work underscores the importance of using temperature-dependent absorption cross sections to accurately model hot exoplanet atmospheres and highlights the need for additional high-temperature VUV data to improve simulations and better represent actual planetary conditions.

A.C. thanks the Université Paris Cité (UPC) for funding support (doctoral grant). Z.P. and O.V. acknowledges funding from the ANR project 'EXACT' (ANR-21-CE49-0008-01). This work is supported by the Centre National d'Etudes Spatiales (CNES). Finally, we thank the organizers of the SF2A 2025.

References

Al-Refaie, A. F., Changeat, Q., Venot, O., & Tinetti, G. 2024, Astrophysical Journal, 681, A33
Fleury, B., Poveda, M., & Bénilan, Y. 2025, Astronomy and Astrophysics, 693, A82
Fortney, J. J., Marley, M. S., Lewis, N. K., & Morley, C. V. 2019, Astrophysical Journal, 880, L16
Gardner, J. P., Mather, J. C., Abbott, R., et al. 2023, PASP, 135, 068001
Heays, A. N., Bosman, A. D., & van Dishoeck, E. F. 2017, Astronomy and Astrophysics, 602, A105
Rauer, H., Aerts, C., Cabrera, J., et al. 2025, Experimental Astronomy, 59, 26
Rocchetto, M., Waldmann, I. P., Venot, O.and Lagage, P.-O., & Tinetti, G. 2016, APJ
Tinetti, G., Drossart, P., Eccleston, P., et al. 2018, Experimental Astronomy, 46, 135
Venot, O., Bénilan, Y., Fray, N., et al. 2018, Astrophysical Journal, 609, A34
Venot, O., Cavalié, T., Bounaceur, R., et al. 2020, Astrophysical Journal, 634, A78
Venot, O., Fray, N., Bénilan, Y., et al. 2013, Astronomy and Astrophysics, 551, A131